



Cell adhesion and twitching motility influence strong biofilm formation in *Pseudomonas aeruginosa*

Hiral Patel & Devarshi Gajjar

To cite this article: Hiral Patel & Devarshi Gajjar (2022): Cell adhesion and twitching motility influence strong biofilm formation in *Pseudomonas aeruginosa*, Biofouling, DOI: [10.1080/08927014.2022.2054703](https://doi.org/10.1080/08927014.2022.2054703)

To link to this article: <https://doi.org/10.1080/08927014.2022.2054703>

 View supplementary material 

 Published online: 28 Mar 2022.

 Submit your article to this journal 

 View related articles 

 View Crossmark data 



Cell adhesion and twitching motility influence strong biofilm formation in *Pseudomonas aeruginosa*

Hiral Patel and Devarshi Gajjar 

Department of Microbiology and Biotechnology Centre, Faculty of Science, The Maharaja Sayajirao University of Baroda, Vadodara, Gujarat, India

ABSTRACT

In the present study, biofilm formation was quantified in UTI isolates of *Pseudomonas aeruginosa* ($n=22$) using the crystal violet assay and was categorized into; strong ($n=16$), weak ($n=4$), and moderate ($n=2$) biofilm producers. Further experiments were done using strong ($n=4$) and weak ($n=4$) biofilm producers. Biofilm formation was greater in Luria broth followed by natural urine and artificial urine on silicone and silicone-coated latex. Cell adhesion and twitching motility were greater in strong biofilm producers. The presence of thick biofilm with an increased number of dead and total number of cells of strong biofilm producers was observed using CLSM. The concentrations of exopolymeric substances (eDNA, protein, and pel polysaccharide) were high in strong biofilm producers. FEG-SEM visualization of biofilm produced by strong biofilm producers showed more cells encased in thick biofilm matrix than weak ones. Overall results provide evidence for increased cell adhesion and twitching motility in strong biofilm producers.

ARTICLE HISTORY

Received 3 September 2021
Accepted 14 March 2022

KEYWORDS

Biofilm; UTI; strong; twitching motility

Introduction

Pseudomonas aeruginosa is an opportunistic pathogen responsible for causing infections like cystic fibrosis, endocarditis, pneumonia, bacteremia, and Urinary Tract Infections (UTIs) (Shigemura et al. 2006; Gomila et al. 2018). Catheter-Associated Urinary Tract Infections (CAUTIs) contribute significantly to hospital-associated infections (HAIs) (Lara-Isla et al. 2017), which are often persistent due to infections caused by biofilm-forming bacteria. *P. aeruginosa* is the third most common pathogen associated with hospital-acquired CAUTIs (Jarvis and Martone 1992; Djordjevic et al. 2013). In a study from India, *P. aeruginosa* accounted for 15% of all bacterial isolates collected from a tertiary care hospital over a period of 2012 to 2016 (Kumari et al. 2019). Infections caused by *P. aeruginosa* are often difficult to treat since it is resistant to a wide range of antibiotics due to multiple modes of resistance and its ability to form biofilms on medical devices (Lister et al. 2009; Langendonk et al. 2021). UTIs caused by *P. aeruginosa* are associated with high mortality in hospitalized patients (Lamas Ferreira et al. 2017). *P. aeruginosa* biofilms are difficult to eradicate as bacteria embedded in the

matrix are protected from phagocytosis, are resistant to most drugs compared to their planktonic counterparts, and show long-term persistence (Thi et al. 2020). The biofilm-forming ability of *P. aeruginosa* is highly associated with its virulence and drug resistance.

The quantitative differences between biofilms formed by clinical isolates are categorized as strong, moderate, and weak biofilm producers (Stepanović et al. 2004). Owing to ease and relatively low cost, the crystal violet (CV) assay has been the most popular assay for the quantification of biofilms (O'Toole 2011; Thibeaux et al. 2020). A strong biofilm producer forms a thicker biofilm due to the presence of a high number of bacteria (either dead or alive or both) and the increased production of exopolymeric substances (Luther et al. 2018; Suriyanarayanan et al. 2018; Desai et al. 2019). Though several methods are available for biofilm quantification (Corte et al. 2019; Kragh et al. 2019), the CV assay is preferred, as it stains both live and dead cells, as well as the matrix and can be used as a primary indicator of biofilm-forming ability. The importance of distinguishing a strong biofilm producer from a weak biofilm producer can be linked to

CONTACT Devarshi Gajjar  devarshimistry@yahoo.com

 Supplemental data for this article is available online at <https://doi.org/10.1080/08927014.2022.2054703>.

© 2022 Informa UK Limited, trading as Taylor & Francis Group

their ability to survive in harsh conditions. For instance, increased amounts of matrix polymeric substances act as a shelter to protect the encased bacteria and dead cells in strong biofilms provide the necessary biomolecules for the remaining cells to survive (Webb et al. 2003; Ryder et al. 2007).

The composition of *P. aeruginosa* biofilms is well characterized in typed strains (PAO1 and PA14) and has been reviewed extensively (Mulcahy et al. 2014; Thi et al. 2020). The biofilm comprises an extracellular matrix having polysaccharides (alginate, pel, and psl), proteinaceous components, and extracellular DNA (eDNA). Studies on biofilm formation by *P. aeruginosa* in a CAUTI –murine model has shown biofilm formation can be mediated by eDNA even in the absence of exopolysaccharide (Cole et al. 2014). The biofilm matrix protein CdrA binds to pel and psl exopolysaccharides which increases the stability of biofilm (Reichhardt et al. 2018, 2020). The prevalence of *P. aeruginosa* in biofilms formed by bacteria on catheters has been documented (Xu et al. 2015; Tellis et al. 2017; Almalki and Varghese 2020) but a comparative analysis of the differences in the matrix components and biofilm-forming potential of these isolates are lacking.

The present study aimed to quantitate the differences in the biofilm-forming potential of *P. aeruginosa* isolates from UTIs. Further, biofilm formation on various catheters, adhesion, twitching motility, and arrangement of live-dead cells within the biofilm in strong and weak biofilm-producing isolates was also investigated.

Materials and methods

Bacterial cultures and growth conditions

All *P. aeruginosa* isolates were collected from the Sterling and Toprani pathology lab from Vadodara, Gujarat, India. *P. aeruginosa* isolates ($n = 22$) were isolated from UTIs and maintained by subculturing on Pseudomonas Isolation Agar (PIA). Identification of isolates as *P. aeruginosa* was carried out using biochemical tests and 16S rRNA gene sequencing (data not shown)

Biofilm assay

Biofilm quantification of UTI-causing *P. aeruginosa* ($n = 22$) and PAO1 was done using the crystal violet assay (Stepanović et al. 2004). Briefly, in a 96-well microtiter plate, 20 μ l of overnight grown culture (0.2 OD at 600 nm) and 230 μ l LB (Luria Broth) were

mixed and further incubated at 37°C for 24 h under static conditions. The next day, planktonic cells were removed and the biofilm was washed twice with normal saline, fixed with methanol for 15 min, and stained with 0.1% crystal violet (CV) for 15 min. The plates were air-dried for 15 min after being washed. The bound CV was dissolved in 33% glacial acetic acid and quantified spectrophotometrically at 570 nm. Based on cut-off O.D., isolates were classified as strong, moderate, and weak biofilm producers (Stepanović et al. 2004). The cut-off OD (OD_c) value was determined as three standard deviations above the mean OD of the negative control. Isolates were classified as no biofilm producer ($OD \leq OD_c$), weak biofilm producers ($OD_c < OD < 2 \times OD_c$), moderate biofilm producers ($2 \times OD_c < OD < 4 \times OD_c$), and strong biofilm producers ($4 \times OD_c < OD$). All the experiments were carried out in triplicate.

Growth curve

The growth curve was done for strong (ST-20, TP-25, TP-35, and TP-48) and weak (ST-22, TP-8, TP-10, and TP-11) biofilm producers using HT microtiter plate reader (Biotek Instruments, Winooski, VT, USA). 100 μ l of bacterial culture (OD at 600 nm \sim 0.05) was inoculated in a sterile 96-well flat-bottom microtiter plate and incubated at 37°C for 24 h. The optical density (OD) measurement was continuously measured at an interval of 15 min for 12 h until the culture reached to stationary phase. The growth curve was plotted and the growth rate was determined for each strain.

In vitro biofilm quantification on catheters

Experiments to examine biofilm quantification on catheters (silicone-coated latex and silicone catheters) were performed using four strong (ST-20, TP-25, TP-35, and TP-48) and weak (ST-22, TP-8, TP-10, and TP-11) biofilm producers. A 1 cm long piece of the catheter was cut vertically into 2 pieces, sterilized in methanol, and then air-dried. The catheter pieces were kept in a 24 well plate with 2 ml of 1:10 diluted (0.2 OD at 600 nm) culture and incubated at 37°C for 24 h. The amount of biofilm formed was quantified using a modified CV assay. The catheter was placed in a new plate, fixed with methanol for 15-min, stained with 0.1% CV; unbound CV was washed away twice with 0.85% NaCl, the plate was air-dried, bound CV was dissolved in 33% glacial acetic acid and CV was measured spectrophotometrically at

570 nm. Biofilm formed in the presence of Luria broth (LB), Natural Urine (NU) (obtained from a healthy volunteer, filter sterilized through a 0.2 μm filter, and stored at -20°C for further use) and Artificial urine (AU) (composition: 2.43% urea, 1% NaCl, 0.6% KCl, 0.64% Na_2HPO_4 , 0.05 mg mL^{-1} albumin, pH 7) were quantified using the same assay. For negative controls: LB, NU, and AU catheters without bacterial culture were used respectively. The experiment was performed in triplicate for each strain.

Light microscopy

The adhesion ability of the above-mentioned strong ($n = 4$) and weak ($n = 4$) biofilm producers was examined. Briefly, 5 ml of 1:10 diluted bacterial culture (0.2 OD at 600 nm) in LB medium was inoculated in 6 well plates with coverslips and incubated at 37°C for 4 h under static conditions. After incubation, the unbound cells were washed off with 0.85% NaCl, Gram-stained, and observed under a microscope (BX 51 Olympus microscope, Japan) at 100X magnification. The number of cells adhered to the coverslip was counted using Fiji software.

Twitching motility

Twitching motility for previously mentioned strong ($n = 4$) and weak ($n = 4$) biofilm-producers was determined on 1% Luria agar (LA) plates by inoculating and incubating them at 37°C for 24 h followed by measuring the twitching zone (Darzins 1993). Further confirmation of twitching motility was done by phase-contrast time-lapse microscopy. Briefly, twitching motility was observed by spotting 1 μl (0.2 OD at 600 nm) of bacterial culture on a 1% LA pad (we ensured that the LA pad was air-dried). The twitching motility was observed for 4 h and 24 h. The experiment was done in biological triplicates.

Gene expression quantification of type 4 pili and *cdr A* gene

The levels of expression of type 4 pili and biofilm matrix protein Cdr A genes listed in the [supplementary data](#) (Table S1) were analyzed from 4 h to 24 h old biofilms. RNA extraction was carried out using a Nucleospin RNA kit (Macherey Nagel, Hoerd, France). RNA integrity was checked on 2% gel and quantification was done using a Nanodrop (Thermo Fisher Scientific, Waltham, MA, USA). First-strand

cDNA synthesis was performed using a prime 1st Strand cDNA synthesis kit (Takara, Bio Inc, Japan). The qPCR cycling conditions were as follows 95°C for 5 min and 40 cycles of 30 s at 95°C , 30 s at 57°C . Relative quantification was carried out from three independent biological replicates. Data were normalized to rpo D gene expression and fold changes were calculated according to the $2^{-\Delta\Delta\text{Ct}}$ method. The fold change of strong biofilm producers was normalized to weak biofilm producers.

Confocal laser scanning microscopy (CLSM)

Using a Carl Zeiss CLSM 780 and 710 microscope, 24 h old biofilm formed on coverslips in LB medium in 6 well culture plates was examined. Before staining, biofilm was rinsed with 1 ml of 0.85% NaCl to remove planktonic cells. The remaining biofilm attached to the coverslip was stained with Syto 9 and PI dye from LIVE/DEAD[®] BacLight[™] Bacterial Viability Kit for 10 min. The excess stain was gently washed away with 0.85% NaCl. 3D structure of biofilm was captured by CLSM using Z stack. Fiji software was used to measure the live and dead cells in images.

Field emission gun scanning electron microscopy (FEG-SEM)

Strong (TP-25) and weak (TP-8) biofilm producers were cultured in LB for 24 h at 37°C on a silicone-coated latex catheter, as stated above. After incubation, the biofilm was rinsed with sterile PBS (Phosphate Buffer Saline), fixed with 2% glutaraldehyde in PBS at 4°C overnight, then sequentially dehydrated with 30, 50, 70, 90, and 100% ethanol in order. FEG-SEM (Nova Nano SEM 450, FEI Ltd., Hillsboro, OR, USA) was performed in environmental mode.

Quantification of biofilm matrix components

With few modifications, eDNA and extracellular protein quantification were done as described by (Wu and Xi 2009) and normalized with OD 600 nm. In 24 well plates, 2 ml of 1:10 diluted (0.2 at OD 600 nm) culture in LB medium was incubated at 37°C for 24 h. The next day, biofilm was gently rinsed with 0.85% NaCl to remove planktonic cells before being resuspended in 1 ml of 0.85% NaCl. Biofilm was homogenized by vortexing for 30 s and cells were removed by passing it through a 0.22 μm filter. 500 μl of filtered suspension was used for eDNA

quantification and the remaining was used for protein quantification.

eDNA quantification

The eDNA was extracted from 500 μl of filtered solution (above) using the phenol-chloroform method as previously described (Wu and Xi 2009) and quantified by measuring absorbance at 260 nm using nanodrop (Thermo Fisher Scientific, Waltham, MA, USA). The OD at 600 nm was used to normalize the eDNA quantification.

Extracellular protein quantification

Extracellular protein was quantified using a Bradford assay by measuring absorbance at 595 nm in a microtiter plate reader (Multiskan Go, Thermo Fisher Scientific, Waltham, MA, USA). Briefly, 100 μl of filtered solution was added to 1000 μl of Bradford reagent and incubated at room temperature for 10 min. Absorbance was measured at 595 nm.

Pel polysaccharide quantification

The amount of Congo red that binds to Pel-dependent EPS was assayed as described by Madsen et al. 2015 (Madsen et al. 2015). Briefly, 1:10 diluted (0.2 OD at 600 nm) overnight grown culture was inoculated in 2 mL LB and incubated at 37 °C for 24 h. Bacterial content along with EPS was pelleted by centrifugation, resuspended in 40 mg mL^{-1} Congo red in 1% LB and incubated for 2 h at 37 °C at 250 rpm. After 2 h, EPS was pelleted *via* centrifugation and the absorbance of the supernatants of each suspension was measured at 490 nm. 1% LB with 40 mg mL^{-1} Congo red was used as a blank.

Alginate quantification

Alginate extraction was carried out following the protocol by Jones et al., 2013 (Jones et al. 2013). Briefly, a 24 h bacterial colony was scraped off the plate, resuspended in 0.85% NaCl, and collected by centrifugation ($12,000 \times g$ for 30 min). The supernatant was treated with 2% Cetyl Pyridium chloride and alginate was collected by centrifugation. The pellet was resuspended in 1 ml of 1 M NaCl, precipitated with cold isopropanol, and resuspended in normal saline. Alginate quantification was determined by carbazole assay (Cesaretti et al. 2003) with 96 well format modifications (Knutson and Jeanes 1968). 50 μl

of resuspended alginate was treated with a 200 μl borate-sulfuric acid reagent (10 mM H_3BO_3 in concentrated H_2SO_4) at 100 °C for 15 min. Further, 50 μl of carbazole reagent (0.1%) was added and heated to 100 °C for 10 min. Absorbance was measured at 550 nm (Multiskan Go, Thermo Fisher Scientific, Waltham, MA, USA). Seaweed alginate was used as a standard to determine the concentration of alginate.

Pyocyanin quantification

Pyocyanin production by strong ($n=4$) and weak ($n=4$) biofilm producers were determined as described by (Essar et al. 1990). Briefly, overnight grown culture was 1:10 diluted (0.2 OD at 600 nm) and inoculated in 2 ml LB medium and kept shaking at 37 °C for 24 h. The next day, the culture was centrifuged, pyocyanin was extracted from the supernatant with 3 ml chloroform and then re-extracted with 0.2 N HCl. By measuring absorbance at 520 nm and multiplying it by 17.072, the concentration can be expressed as a microgram of pyocyanin produced per ml of supernatant. The OD at 600 nm was used to normalize the concentration. The experiment was performed in triplicate using a blank of 0.2 N HCl.

Rhamnolipid quantification

In LB, 1:10 diluted (0.2 OD culture at 600 nm) overnight grown culture was inoculated and kept at 37 °C for 24 h. Four ml of the supernatant pH was adjusted to 2.3 ± 0.2 using 1 N HCl and extracted with 5 volumes of chloroform. To 4 ml of chloroform extract, 200 μl of 1 g L^{-1} methylene blue solution (pH of methylene blue was adjusted to 8.6 ± 0.2 by adding 50 mM Borax buffer) and 4.9 ml distilled water was added. The sample was vigorously mixed and kept at room temperature for 15 min. The OD of the chloroform phase was measured at 638 nm and normalized with the $A_{600\text{nm}}$ (Pinzon and Ju 2009). Chloroform was used as blank.

Effect of exogenous treatments (enzymes, eDNA, proteins) on biofilm formation

Enzymatic digestion of biofilm

Biofilm was grown in a 96 well microtiter plate for 24 h at 37 °C as described for the biofilm assay. The next day, planktonic cells were washed off with 0.85% NaCl and the biofilm was treated with 100 $\mu\text{g ml}^{-1}$ of DNase, RNase, and proteinase K each in separate wells and further incubated at 37 °C for 24 h (Tetz

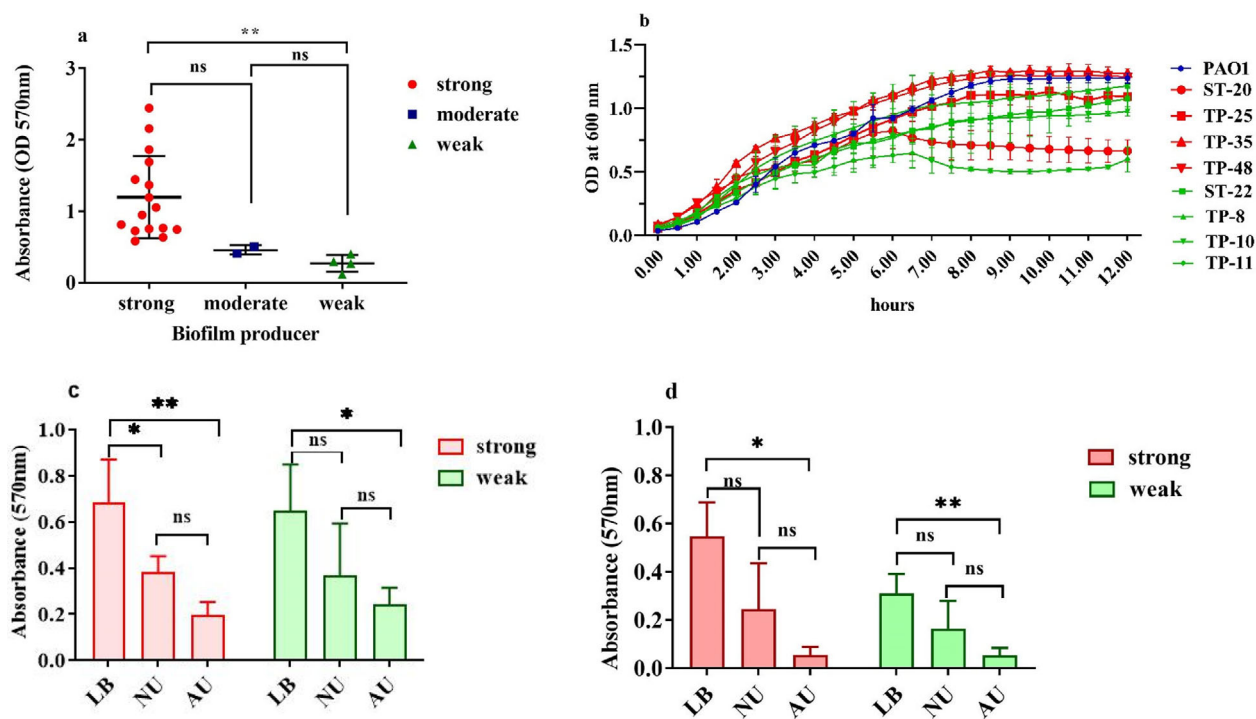


Figure 1. Biofilm Quantification: Biofilm quantification and categorization of UTI isolates of *P. aeruginosa* ($n=22$) into strong, moderate and weak (a). Growth curve of strong (ST-20, TP-25, TP-35, TP-48) and weak biofilm producers (ST-22, TP-8, TP-10, TP-11) (b). Biofilm quantification on silicone-coated latex catheter in presence of LB, NU, AU (c) and silicone catheter in presence of LB, NU, AU (d). The experiment was conducted in three biological replicates for each strain. Error bars indicate standard deviation. Two-way ANOVA was performed for statistical significance were ns $p > 0.05$, * $p < 0.05$, ** $p < 0.005$, *** $p < 0.0005$.

et al. 2009). Following 24h, the biofilm was rinsed with 0.85% NaCl and quantified using the crystal violet assay. LB medium with culture was used as control and sterile LB medium was used as the blank. The experiment was performed in triplicate.

Addition of eDNA and extracellular protein in biofilm

To substantiate the role of eDNA and extracellular protein in biofilm, an addition assay was performed (Harmsen et al. 2010). Biofilm was formed using the above mention protocol with the addition of *P. aeruginosa* extracted eDNA, genomic DNA, and extracellular protein (concentration 100 ng mL^{-1} for DNA and $3 \mu\text{g mL}^{-1}$ for protein) and incubated at 37°C for 24h (Harmsen et al. 2010). The next day, unbound cells were washed off and a CV assay was performed as stated previously. Bacterial culture with LB was used as control and only LB as blank. The experiment was performed in triplicate.

Statistical analysis

Statistical analysis for biofilm formation on catheters was done using the GraphPad Prism 9.0 software with two-way ANOVA. For other experiments

represented by bar graphs and line graphs, student's *t*-test and one-way ANOVA or 2-way ANOVA was applied. Non-parametric data represent the mean \pm standard deviation.

Results

Biofilm categorization of UTI isolates of *P. aeruginosa*

The crystal violet (CV) assay was used to categorize UTI-causing *P. aeruginosa* ($n=22$) isolates into strong, moderate, and weak biofilm producers based on cut-off OD value. The majority of the isolates were found to be strong ($n=16$), while few were moderate ($n=2$) or weak ($n=4$) biofilm producers (Figure 1a). Strong (ST-20, TP-25, TP-35 and TP-48) and weak (ST-22, TP-8, TP-10, TP-11) biofilm producers were randomly selected for all further experiments. The mean growth rate of strong ($n=4$) and weak ($n=4$) biofilm producers was 0.24 ± 0.02 per hour (Figure 1b). One isolate of each strong (ST-20) and weak (TP-11) biofilm producer appeared as slow growers and showed a lower plateau but did not attain statistical significance (Figure 1b).

Biofilm quantification on catheters

In vitro biofilm quantification was studied on silicone-coated latex and silicone catheters in presence of LB, NA, and AU of strong (ST-20, TP-25, TP-35 and TP-48) and weak (ST-22, TP-8, TP-10, TP-11) biofilm producers. On both catheters, the maximum amount of biofilm formation was observed on LB followed by NU and AU by strong and weak biofilm producers (Figure 1c-d). There was no difference in biofilm formation by strong biofilm producers on silicone-coated latex compared to silicone catheters irrespective of the medium used (Figure S1a). Within weak biofilm producers, the highest biofilm formation was observed on silicone-coated latex catheters compared to silicone in the presence of LB (Figure S1a). Negligible differences were observed in NU and AU (Figure S1a). Further, the maximum amount of biofilm formation was observed by strong biofilm producers compared to weak biofilm producers on silicone catheters in LB (Figure S1b). Whereas no difference was observed in biofilm formation by strong and weak biofilm producers on both catheters irrespective of the medium used (Figure S1b).

Adhesion assay and twitching motility

The cell adhesion ability of strong and weak biofilm producers was examined on coverslips after 4 h of incubation. Adhesion by strong biofilm producers showed a greater number of cells adhered to the coverslip compared to weak biofilm producers in light microscopy images (Figure 2a). The number of cells adhered to the coverslip was significantly high in strong ($n = 727 \pm 100$) biofilm producers when compared with weak ($n = 127 \pm 29$) biofilm producers (Figure 2b). Type 4 pili (T4P) mediated twitching motility is essential for surface attachment and the initial stage of microcolony formation.

The twitching motility of PAO1 and strong and weak biofilm producers on 1% LA plates was examined (Figure 2c). A significant difference was observed between the twitching zone of strong (1.1 ± 0.40 mm) and weak (0.6 ± 0.21 mm) biofilm producers (Figure 2d). Further, in phase-contrast time-lapse microscopy, a greater number of twitching cells were observed at 4 h in strong biofilm producers (Video S1- upper panel). In contrast, the twitching of cells was less in weak biofilm producers (Video S1 - lower panel). One isolate namely TP10 (weak biofilm producer) completely lacked twitching motility (Video S1—lower panel TP10). As a consequence of greater twitching in strong biofilm producers, the wrinkly edge formation

was observed at 24 h (Figure 2e, upper panel). The fully wrinkly colony edge formation was absent in weak biofilm producers (Figure 2e, lower panel). The quantification of gene expression for the T4P gene was done at 4 h and 24 h biofilms. The type 4 pili expression was 5-fold more compared to weak biofilm producers at 4 h (Figure 2f), and 3-fold high at 24 h (Figure 2f).

Microscopy of biofilm

The biofilm formed on the coverslips by strong and weak biofilm producers was visualized by CLSM using Syto and PI dyes. The arrangements of live and dead cells within the biofilms formed by strong and weak biofilm producers can be viewed in the orthogonal plane (Figure 3 a and c). The biofilm formed by strong biofilm producers had less live cells and a greater number of dead cells as observed in the orthogonal plane (Figure 3a). While biofilm formed by weak biofilm producers had more live cells except for one isolate (TP-11) (Figure 3c) in which excess cell death was observed. This could be because of more pyocyanin production (in TP11), as pyocyanin-mediated cell death is reported in *P. aeruginosa* (Das and Manefield 2012). Further, the YZ and XZ planes of Figure 3a and c showed the variation across the thickness in biofilms formed by strong ($31.25 \mu\text{m} \pm 14.3$) and weak ($19.05 \mu\text{m} \pm 9$) biofilm producers (Figure 3 a and c). The tiled images of strong biofilm producers show tightly packed cells (Figure 3 b) whereas in weak biofilm producers, cells are loosely distributed across the substratum (Figure 3 d). Representative supplementary video S2 shows a clear arrangement of live and dead cells within the biofilm. Biofilms formed by strong biofilm producers are densely packed with dead bacteria confined near the substratum, whereas live cells are scarce and positioned above dead cells (Supplementary Video S2-upper panel). However, the biofilm formed by weak biofilm producers differs in arrangements of live and dead cells. The biofilm formed by weak biofilm producers (ST-22 and TP-10) had more live cells near the substratum than dead cells (Supplementary Video S2-lower panel). Additionally, the number of dead and live cells in each slice of Z stack from strong ($n = 4$) and weak ($n = 4$) biofilm producers were determined. Cell counts (total and dead) show significant differences between strong ($n = 4$) and weak ($n = 4$) biofilm producers (Figure 3e).

FEG-SEM at 3000X resolution of biofilm formed on silicone-coated latex catheter in the presence of LB

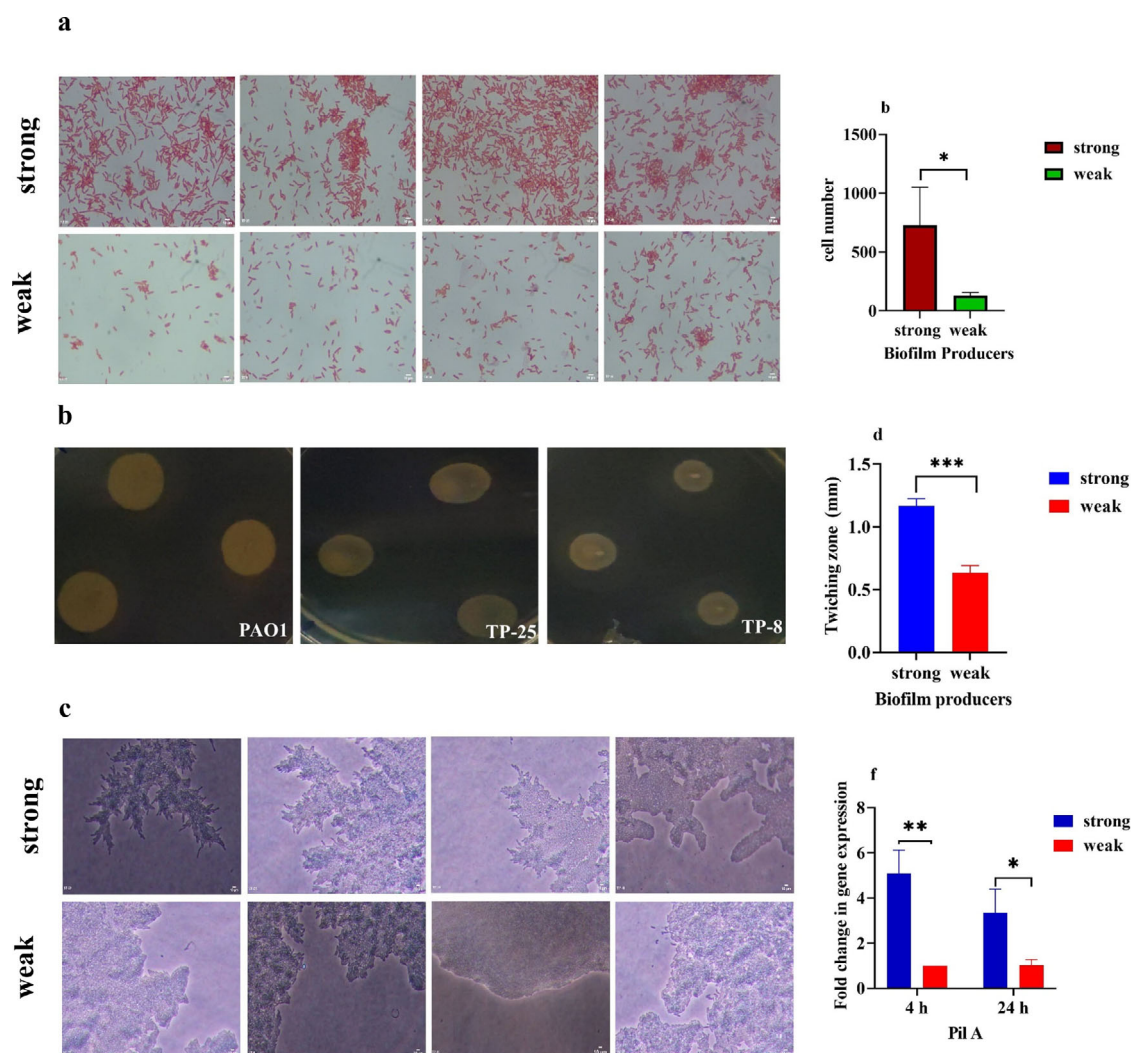


Figure 2. Cell adhesion and twitching motility: Representative images of light microscopy of strong (ST-20, TP-25, TP-35, TP-48) and weak (ST-22, TP-8, TP-10, TP-11) biofilm producers adhered to coverslip at 4 h incubation (a). Cell count of adhesion assay (b). Twitching motility zone of PAO1, strong (TP-25) and weak (TP-8) biofilm producers on 1% LA pad (c). Twitching zone diameter of strong and weak biofilm producers (d). Phase-contrast microscopy of colony edge formation at 24 h of strong ($n=4$) and weak ($n=4$) biofilm producers (e). Pil A gene expression of strong and weak biofilm producers at 4 h and 24 h. All experiments were performed in triplicate for each isolate (f). Statistical significance from student *t*-test were * $p < 0.5$, ** $p < 0.05$, *** $p < 0.005$. Scale bar indicates 10 μ m.

medium shows that strong (TP-25) produced thick biofilm (Figure 4a upper left panel). Due to the EPS, bacteria were not visible at 3000X in the biofilm formed by a strong biofilm producer. On the other hand, biofilm formed by weak biofilm producers had a thin layer of bacteria adhered to the catheter and less EPS (Figure 4b upper right panel). Increased magnification to 6000X showed rod-shaped cells encased within the EPS matrix of biofilm formed by strong biofilm producer (Figure 4a; middle left panel); whereas in biofilm formed by weak biofilm producers, cells are adhered to the catheter as well as to each other and EPS production is hardly observed (Figure 4b; middle right panel). Further magnification to 12000 X, also confirmed that cells are encased in EPS

of strong biofilm producer (Figure 4a lower left panel) and the EPS looked like a dense mass with an irregular surface. While in weak biofilm producers, cells aggregated and microcolony formation was barely observed (Figure 4b; lower right panel).

Components of biofilm

The difference in biofilm components: eDNA, an extracellular protein, pyocyanin, rhamnolipid, pel, and alginate exopolysaccharide was measured for biofilms formed by strong ($n=4$) and weak biofilm producers ($n=4$). The amount of eDNA was $265 \pm 130 \mu\text{g}$ at OD600 in strong biofilm producers and it was $44.96 \pm 11.45 \mu\text{g}$ at OD600 weak biofilm producers

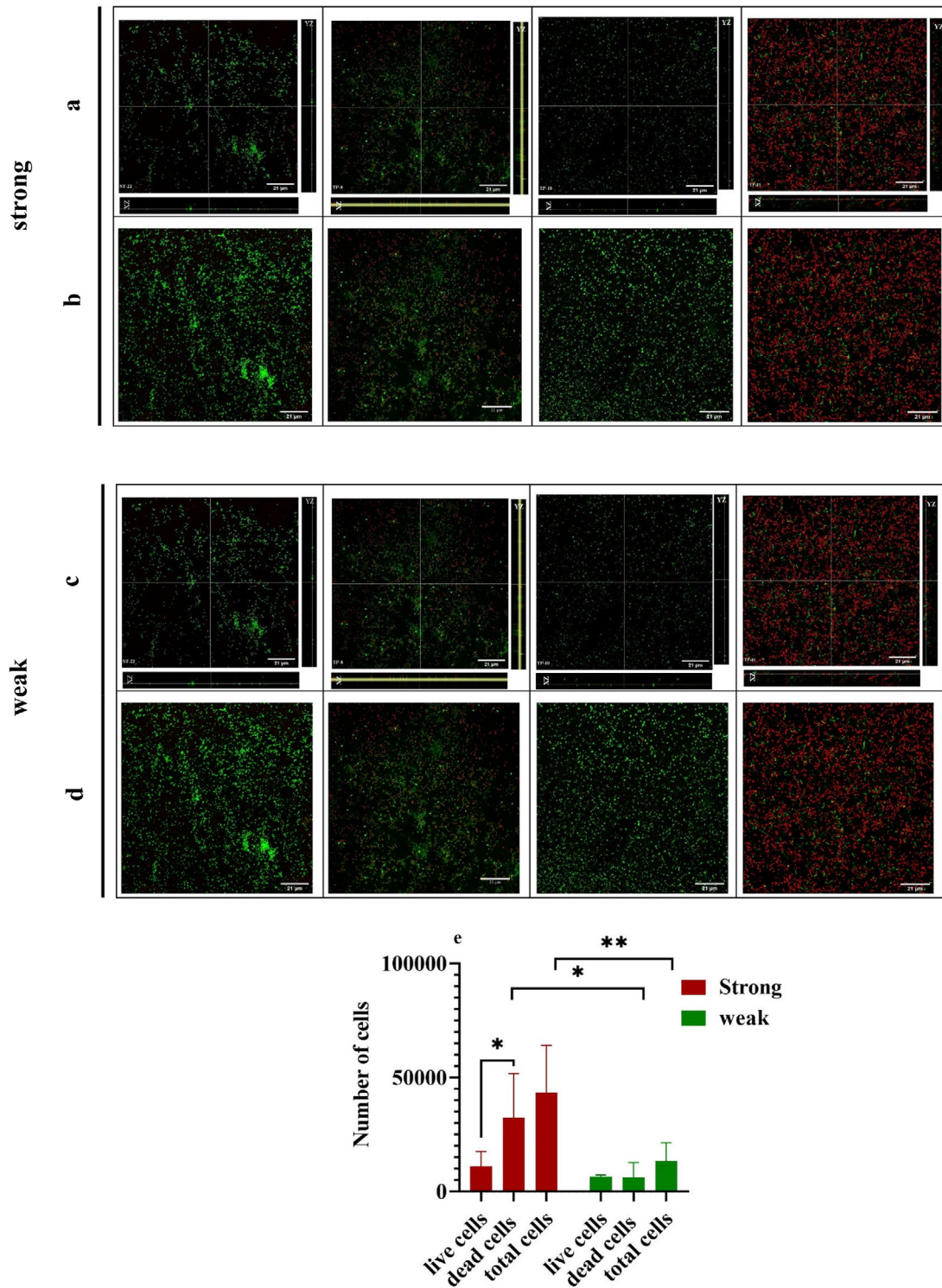


Figure 3. Confocal laser scanning microscopy (CLSM) of biofilms formed by strong and weak biofilm producers: Biofilm formed by strong (ST-20, TP-25, TP- 35, TP-48) and weak (ST-22, TP-8, TP- 10, TP-11) biofilm producers on coverslip after 24 h were subjected to CLSM after staining with Syto9 (green – live cells) and PI (red – dead cells) (a, b, c, and d). Representative images of orthogonal view of Z-stack strong (a-) and weak (c-) biofilm producers, tiled images of strong (b) and weak (d) biofilm producers. Cell counts of living, dead, and total cells (dead and live) within the Z-stack of strong and weak biofilm producers (e). One-way ANOVA was carried out for statistical significance were ns $p > 0.05$, * $p < 0.05$, ** $p < 0.005$. Scale bar indicates 21 μm .

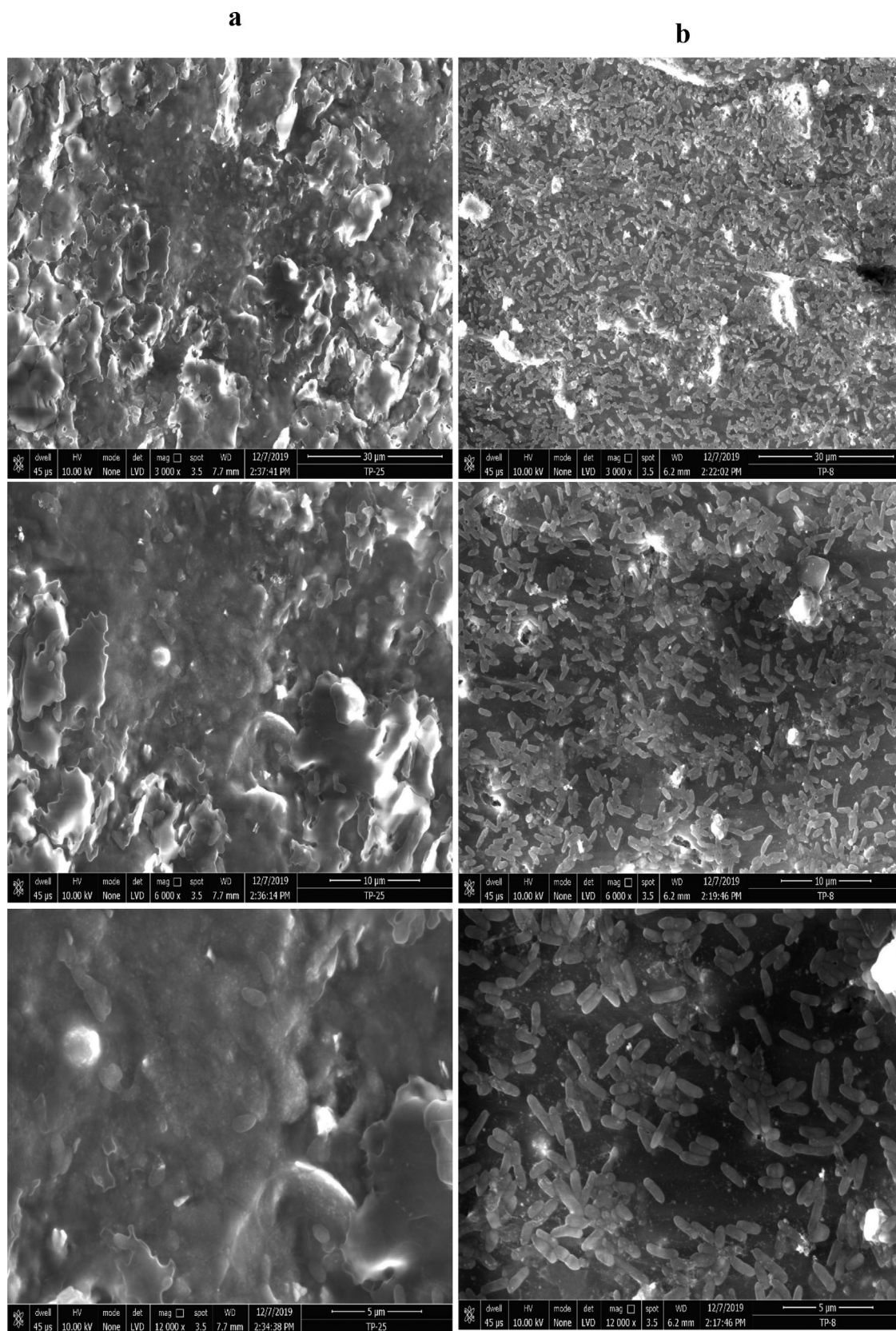


Figure 4. FEG-SEM of biofilm: Representative images of biofilm formed by strong (TP-25) (a) and weak (TP-8) (b) biofilm producers on silicone-coated latex catheter at 3000X (upper panel), 6000X (middle panel), and 12000X (lower panel) magnifications. Scale bar indicates 30 μ m, 10 μ m, 5 μ m.

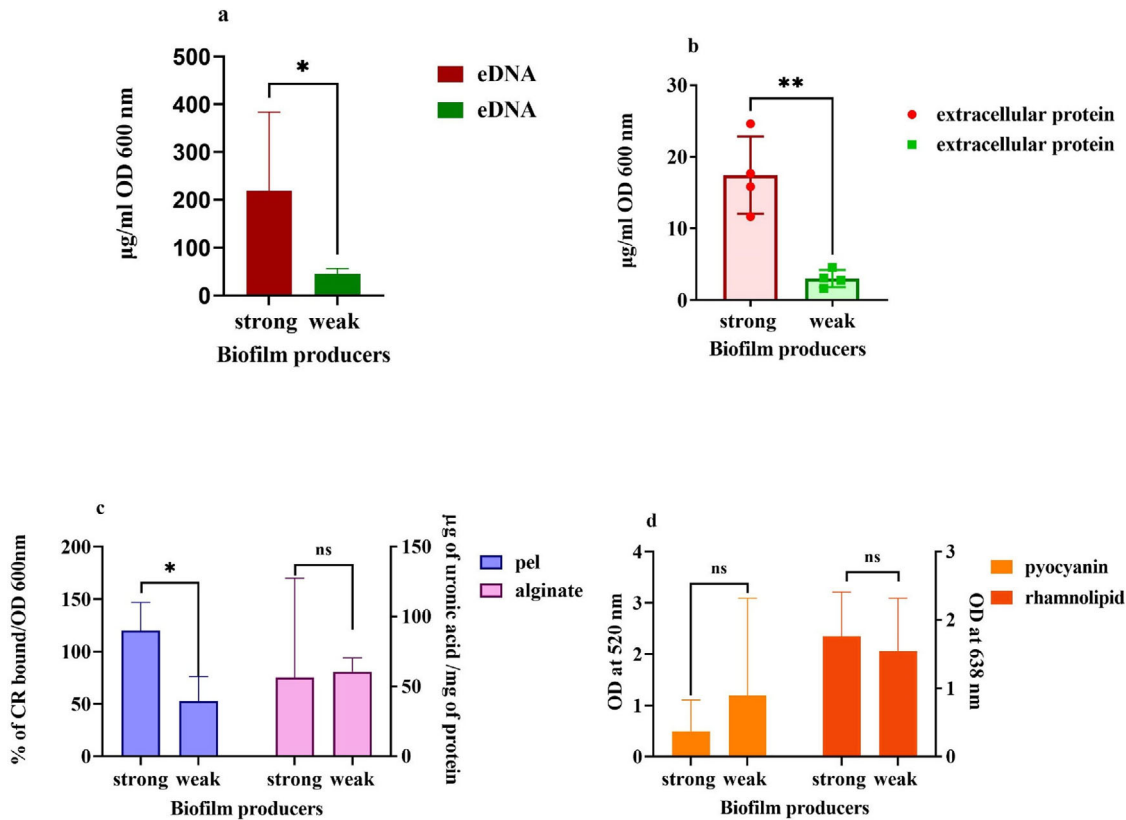


Figure 5. Quantification of biofilm matrix components: eDNA (a), extracellular protein (b) pel and alginate exopolysaccharide (c), rhamnolipid and pyocyanin (d). Error bar indicates standard deviation. Student *t*-test carried out for statistical significance were ns $p > 0.05$, * $p < 0.05$, ** $p < 0.005$.

(Figure 5a). The extracellular protein quantified in biofilm formed by strong biofilm producers ($17.45 \pm 5.30 \mu\text{g}$ at OD600) was also significantly higher than weak biofilm producers ($3.04 \pm 1.20 \mu\text{g}$ at OD600) (Figure 5b). The concentration of pel exopolysaccharides was significantly higher in strong biofilm producers ($120.10 \pm 26.79 \mu\text{g}$ at OD600) than weak biofilm producers ($52.83 \pm 23.38 \mu\text{g}$ at OD600) (Figure 5c). There was no significant difference between strong and weak biofilm producers in the case of alginate exopolysaccharide, pyocyanin, and rhamnolipid (Figure 5c-d).

Effect of exogenous treatments (enzymes, eDNA, proteins) on biofilm formation

The effect of enzymatic treatments (DNase I, proteinase K, and RNase) on biofilm formation by strong biofilm producers showed the greatest inhibition by proteinase K treatment, followed by RNase and DNase treatment that reduced biofilm by 76.35%, 63.43%, and 43.35%, respectively (Figure 6a). Out of the three treatments, only the DNase treatment resulted in a significant reduction of biofilm (58.27%) in weak biofilm producers (Figure 6a). Further, the

addition of exogenous DNA and extracellular protein may increase the amount of biofilm. A decrease in biofilm was observed in both strong and weak biofilm producers upon the addition of eDNA when compared to control (no eDNA is added) (Figure 6b). No significant difference was observed with the addition of extracellular protein in comparison to the control (no extracellular protein added) (Figure 6c)

Discussion

The first objective in the present study was to determine whether the UTI isolates of *P. aeruginosa* had any differences in their biofilm-forming abilities. The majority of isolates were strong biofilm producers with negligible differences in biofilm formation between silicone and silicone coated catheters; all isolates showed levels of biofilm production on catheters in order of LB > NU > AU medium. Similar results were observed by Vipin et al., 2019 who showed that weak biofilm producers form strong biofilms on silicone-coated latex catheters in tryptone soya broth (Vipin et al. 2019). The porous surface of silicone-coated latex catheters was shown to enhance biofilm formation due to the high adhesion of bacteria (Lee

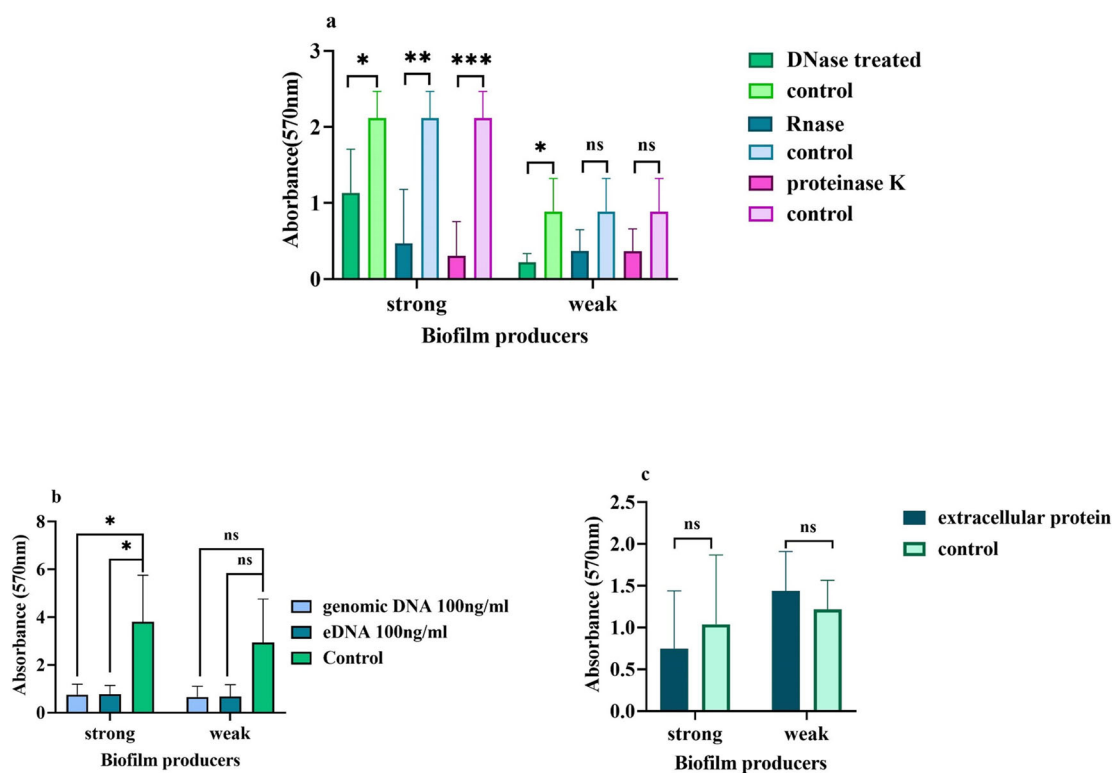


Figure 6. Effect of exogenous treatments (enzymes, eDNA, proteins) on biofilm formation: Effect of DNase I, RNase and proteinase K (a); Addition of eDNA and genomic DNA (b); addition of extracellular protein (c). Statistical significance carried out using student *t*-test were ns $p > 0.05$, * $p < 0.05$, ** $p < 0.005$, *** $p < 0.0005$.

et al. 2017), while silicone catheters have a smooth surface and are known to reduce cell adhesion (Feneley et al. 2015). In a recent study, *P. aeruginosa* exhibited significantly high biofilm when cultured on a 96-well polystyrene plate (hydrophobic surface) and glass surface in the presence of LB medium (Asghari et al. 2021). A limitation of the study is that the entire study is based on the initial categorization of biofilm formation into strong and weak biofilm producers using the CV assay in 96 well polystyrene plates. CV staining probes all components of the biofilm (i.e. live-dead cells, proteins, RNA, eDNA, polysaccharides, etc.) and so it was used as a preliminary indicator. Later, microscopy (light, CLSM, and SEM) and biochemical assays were done to find the differences between biofilms formed by strong and weak biofilm producers. Hence, glass coverslips were used for adhesion assays and CLSM imaging, while silicone-coated latex catheters were used for SEM. Many variables like surface properties, cell surface hydrophobicity, medium, cell appendages (flagella and T4P) (Zheng et al. 2021) could contribute to the diverse behaviour of clinical isolates. Diverse behaviour is also reported for isolates causing cystic fibrosis (Deligianni et al. 2010). Only 54% of keratitis causing *P. aeruginosa*

isolates showed biofilm formation (Heidari et al. 2018). Most studies on *P. aeruginosa* from UTI have focused on antibiotic resistance (Saxena et al. 2014; Kamali et al. 2020; Mirzahosseini et al. 2020) and reports on the quantification of biofilm formation by clinical isolates of *P. aeruginosa* causing UTIs are scanty.

The differences in biofilms formed by clinical isolates could be due to their differences in twitching motility, adhesion and/or components of the biofilm matrix. Cell adhesion, twitching motility, and expression of *pilA* gene were higher in strong biofilm producers. The importance of type 4 pili (T4P) mediated twitching motility as a means of initiating contact on abiotic surfaces and biofilm formation is well documented (O'Toole and Kolter 1998; Pratt and Kolter 1998; Mattick 2002). In a study on clinical and environmental isolates, it was found that when the motility phenotype was present, there was a notable increase in biofilm (Head and Yu 2004; Inclan et al. 2011). Differences in biofilm formation and variations in biofilm morphology amongst clinical isolates ($n = 5$) from cystic fibrosis patients were correlated with motility and it was concluded that though motility is not an absolute requirement for biofilm formation it

does contribute to the formation of thick biofilms (Deligianni et al. 2010). In a recent study of 190 clinical isolates of *P. aeruginosa*, twitching motility was strongly associated with high biofilm formation while isolates with high swimming and swarming motility failed to produce a strong biofilm (Horna et al. 2019). The biogenesis, functioning, and regulation of T4P mediated twitching motility is well characterized and several complex systems control the T4P responses. Hence, prediction of T4P behavior in response to diverse cues is difficult. The two major determinants of the motility–sessility switch in *P. aeruginosa* are the cellular levels of c-di-GMP or cAMP, and levels of both have shown to increase during growth on solid media (Hengge 2009; Römling et al. 2013; Valentini and Filloux 2016). Levels of c-di-GMP and cAMP are adjusted in response to extracellular signals received by several sensing systems (WspA, WspR, Gac-Rsm, RocS1) and chemotactic cluster (PilGHJK-ChpABC) respectively (Chang 2017). In a recent study, T4P mediated motility was shown to cause biofilm expansion in response to host-derived signals, serum albumin (known to be present in urine) and mucin (elevated in lungs of cystic fibrosis patients). BSA, mucin, and tryptone were shown to elevate levels of T4P and cAMP via ChpC (Nolan et al. 2020). The same study also showed that secreted protease activity may be required for liberating components from mucin, BSA, and tryptone that stimulate twitching motility and that a small quantity of this component is present in tryptone that does not require protease activity to get liberated. High biofilm formation in LB was observed (tryptone: 10 g L⁻¹); hence it is hypothesized that the presence of tryptone could increase the amount of cAMP thereby causing strong biofilm formation. On the other hand, the presence of urea in natural and artificial urine may inhibit quorum sensing due to which biofilm formation was less in presence of urine (Cole et al. 2018). Overall, a vast range of environmental and host signals have been shown to stimulate twitching and these signals along with the genomic diversity of clinical isolates lead to differences in biofilm formation among clinical isolates of *P. aeruginosa*.

Increased cell death, eDNA, an extracellular protein, and pel polysaccharide in biofilms formed by strong biofilm producers was observed. Association of cell death with eDNA in *P. aeruginosa* biofilms is very well established and cell death in *P. aeruginosa* biofilms is considered analogous to programmed cell death in eukaryotes. The considerable amount of DNA in the biofilm matrix is mediated due to cell

autolysis in microcolonies (Webb et al. 2003). Pel is a cationic exopolysaccharide produced by *P. aeruginosa*, and it has been shown to cross-link extracellular DNA in the biofilm matrix to provide stability and structural integrity to the biofilm (Jennings et al. 2015). Mechanisms of cell death and eDNA release have been reviewed recently (Sarkar 2020). These include; membrane damage (caused due to quorum sensing molecules and pyocyanin production), lambda prophage induction and reinfection, ROS production and PQS mediated Phz A-G expression. One of many of the above mechanisms could contribute to cell death and eDNA in biofilms. Hence, further studies to clarify the possible involvement of the above pathways for cell death are warranted using the clinical isolates. Increased production of pyocyanin in TP-11 (weak biofilm producer) may be responsible for increased cell death. It appears that cell death alone may not contribute to strong biofilm formation. One limitation of this study is that exopolysaccharide Psl was not measured. The exopolysaccharide Psl is cell-surface associated and functions as an adhesin in the initial phase of biofilm formation, but relocates as a peripheral exopolysaccharide at later stages of biofilm formation (Ma et al. 2009). *P. aeruginosa* isolates with the pel and psl genes had more robust biofilms than strains deficient in these genes; in a murine model, cell lysis is mediated by urea, and biofilm formation is independent of exopolysaccharides (Cole et al. 2014).

The cdr A is the only well-characterized extracellular protein (Reichhardt et al. 2020) and in the present study, no difference was found in the expression of cdr A when compared between strong and weak biofilm producers (data not shown). It is possible that the protein content in the matrix is highly dynamic and consists of many proteins. A study using iTRAQ-based quantitative proteomics to evaluate matrix-associated proteins isolated from different phases of *P. aeruginosa* ATCC27853 biofilms showed that 54 different proteins varied from time to time during biofilm formation (Zhang et al. 2015). This warrants further studies on extracellular proteins in biofilms caused by *P. aeruginosa* in CAUTIs.

Based on these results, high adhesion ability and twitching motility contribute to strong biofilm formation. Weak biofilm-producing isolates showed good diversity. Since biofilms are difficult to eliminate, twitching motility and high adhesion ability found in the early stages of biofilm formation can be exploited as therapeutic targets for biofilm formation.

Acknowledgments

We would like to acknowledge “Confocal Laser Scanning Microscopy (Carl Zeiss LSM 780) Central Facility of IRCC” housed in the BSBE Department of IIT-Bombay. we also acknowledge “Confocal Laser Scanning Microscopy (Carl Zeiss LSM 710) housed in Central Facility at VSI-CMB Department of MSU Baroda”. We thank the Sophisticated Instrumentation Centre for Applied Research and Testing-SICART, Vallabh Vidyanagar for their Scanning Electron Microscope (SEM) facility.

Disclosure statement

The authors declare no conflict-of-interest disclosure.

Supplementary material

Table S1: Primers used in the study for Pili A and Cdr A gene expression in strong and weak biofilm forming isolate.

Supplementary Figure S1: Statistical comparison of biofilm formation by strong and weak biofilm producers (a and b). The Experiment was conducted in three biological experiments for each strain. Error bar indicates standard deviation. Two-way ANOVA was performed for statistical significance were ns $p > 0.05$, * $p < 0.05$, ** $p < 0.005$, *** $p < 0.0005$.

Supplementary video S1: Twitching motility of strong and weak biofilm producers at 4 h on 1% LA pad.

Supplementary video S2: CLSM image of biofilm formed by strong and weak biofilm producers.

Funding

This work was supported by a research grant from Maharaja Sayajirao University of Baroda (RCC/Dir/2017/335/10). Hiral Patel thanks for CSIR-UGC fellowship-University Grants Commission (UGC). We are also grateful for the infrastructure support to this department under the DST-FIST program of the Government of India and Biotechnology- Teaching Programme.

ORCID

Devarshi Gajjar  <http://orcid.org/0000-0002-1330-3823>

References

Almalki MA, Varghese R. 2020. Prevalence of catheter associated biofilm producing bacteria and their antibiotic sensitivity pattern. *J King Saud Univ Sci.* 32:1427–1433. doi:10.1016/j.jksus.2019.11.037

Asghari E, Kiel A, Kaltschmidt BP, Wortmann M, Schmidt N, Hüsgen B, Hütten A, Knabbe C, Kaltschmidt C, Kaltschmidt B. 2021. Identification of microorganisms from several surfaces by maldi-tof ms: *P. aeruginosa* is leading in biofilm formation. *Microorganisms.* 9: 918–992. doi:10.3390/microorganisms9050992

Cesaretti M, Luppi E, Maccari F, Volpi N. 2003. A 96-well assay for uronic acid carbazole reaction. *Carbohydr Polym.* 54:59–61. doi:10.1016/S0144-8617(03)00144-9

Chang C. 2017. Surface sensing for biofilm formation in *Pseudomonas aeruginosa*. *Front Microbiol.* 8:2671. doi:10.3389/fmicb.2017.02671

Cole SJ, Hall CL, Schniederberend M, Farrow JM, Goodson JR, Pesci EC, Kazmierczak BI, Lee VT. 2018. Host suppression of quorum sensing during catheter-associated urinary tract infections. *Nat Commun.* 9:1–8. doi:10.1038/s41467-018-06882-y

Cole SJ, Records AR, Orr MW, Linden SB, Lee VT. 2014. Catheter-associated urinary tract infection by *Pseudomonas aeruginosa* is mediated by exopolysaccharide-independent biofilms. *Infect Immun.* 82:2048–2058. doi:10.1128/IAI.01652-14

Corte L, Pierantoni DC, Tascini C, Roscini L, Cardinali G. 2019. Biofilm specific activity: a measure to quantify microbial biofilm. *Microorganisms.* 7:73. doi:10.3390/microorganisms70300

Darzens A. 1993. The pilG gene product, required for *Pseudomonas aeruginosa* pilus production and twitching motility, is homologous to the enteric, single-domain response regulator CheY. *J Bacteriol.* 175:5934–5944. doi:10.1128/jb.175.18.5934-5944.1993

Das T, Manefield M. 2012. Pyocyanin promotes extracellular DNA release in *Pseudomonas aeruginosa*. *PLoS One.* 7:e46718. doi:10.1371/journal.pone.0046718

Deligianni E, Pattison S, Berrar D, Ternan N, Haylock R, Moore J, Elborn S, Dooley J. 2010. *Pseudomonas aeruginosa* cystic fibrosis isolates of similar RAPD genotype exhibit diversity in biofilm forming ability in vitro. *BMC Microbiol.* 10:38. doi:10.1186/1471-2180-10-38

Desai S, Sanghrajka K, Gajjar D. 2019. High adhesion and increased cell death contribute to strong biofilm formation in *Klebsiella pneumoniae*. *Pathogens.* 8:277. doi:10.3390/pathogens8040

Djordjevic Z, Folic MM, Zivic Z, Markovic V, Jankovic SM. 2013. Nosocomial urinary tract infections caused by *Pseudomonas aeruginosa* and acinetobacter species: sensitivity to antibiotics and risk factors. *Am J Infect Control.* 41:1182–1187. doi:10.1016/j.ajic.2013.02.018

Essar DW, Eberly L, Hadero A, Crawford IP. 1990. Identification and characterization of genes for a second anthranilate synthase in *Pseudomonas aeruginosa*: interchangeability of the two anthranilate synthases and evolutionary implications. *J Bacteriol.* 172:884–900. doi:10.1128/jb.172.2.884-900.1990

Feneley RCL, Hopley IB, Wells PNT. 2015. Urinary catheters: history, current status, adverse events and research agenda. *J Med Eng Technol.* 39:459–470. doi:10.3109/03091902.2015.1085600

Gomila A, Carratalà J, Eliakim-Raz N, Shaw E, Wiegand I, Vallejo-Torres L, Gorostiza A, Vigo JM, Morris S, Stoddart M, COMBACTE MAGNET WP5 RESCUING Study Group and Study Sites, et al. 2018. Risk factors and prognosis of complicated urinary tract infections caused by *Pseudomonas aeruginosa* in hospitalized patients: a retrospective multicenter cohort study. *Infect Drug Resist.* 11:2571–2581. doi:10.2147/IDR.S185753

Harmsen M, Lappann M, Knöchel S, Molin S. 2010. Role of extracellular DNA during biofilm formation by *Listeria*

- monocytogenes. *Appl Environ Microbiol.* 76:2271–2279. doi:10.1128/AEM.02361-09
- Head NE, Yu H. 2004. Cross-sectional analysis of clinical and environmental isolates of *Pseudomonas aeruginosa*: biofilm formation, virulence, and genome diversity. *Infect Immun.* 72:133–144. doi:10.1128/IAI.72.1.133-144.2004
- Heidari H, Hadadi M, Sedigh Ebrahim-Saraie H, Mirzaei A, Taji A, Hosseini SR, Motamedifar M. 2018. Characterization of virulence factors, antimicrobial resistance patterns and biofilm formation of *Pseudomonas aeruginosa* and *Staphylococcus* spp. strains isolated from corneal infection. *J Fr Ophtalmol.* 41:823–829. doi:10.1016/j.jfo.2018.01.012
- Hengge R. 2009. Principles of c-di-GMP signalling in bacteria. *Nat Rev Microbiol.* 7:263–273. doi:10.1038/nrmicro2109
- Horna G, Quezada K, Ramos S, Mosqueda N, Rubio M, Guerra H, Ruiz J. 2019. Specific type IV pili groups in clinical isolates of *Pseudomonas aeruginosa*. *Int Microbiol.* 22:131–141. doi:10.1007/s10123-018-00035-3
- Inclan YF, Huseby MJ, Engel JN. 2011. FimL regulates cAMP synthesis in *Pseudomonas aeruginosa*. *PLoS One.* 6:e15867. doi:10.1371/journal.pone.0015867
- Jarvis WR, Martone WJ. 1992. Predominant pathogens in hospital infections. *J Antimicrob Chemother.* 29:19–24. doi:10.1093/jac/29.suppl_A.19
- Jennings LK, Storek KM, Ledvina HE, Coulon C, Marmont LS, Sadovskaya I, Secor PR, Tseng BS, Scian M, Filloux A, et al. 2015. Pel is a cationic exopolysaccharide that cross-links extracellular DNA in the *Pseudomonas aeruginosa* biofilm matrix. *Proc Natl Acad Sci U S A.* 112:11353–11358. doi:10.1073/pnas.1503058112
- Jones CJ, Ryder CR, Mann EE, Wozniak DJ. 2013. AmrZ modulates *Pseudomonas aeruginosa* biofilm architecture by directly repressing transcription of the *psl* operon. *J Bacteriol.* 195:1637–1644. doi:10.1128/JB.02190-12
- Kamali E, Jamali A, Ardebili A. et al. Evaluation of antimicrobial resistance, biofilm forming potential, and the presence of biofilm-related genes among clinical isolates of *Pseudomonas aeruginosa*. *BMC Res Notes.* 2020;13:27. doi:10.1186/s13104-020-4890-z
- Knutson CA, Jeanes A. 1968. A new modification of the carbazole analysis: application to heteropolysaccharides. *Anal Biochem.* 24:470–481. doi:10.1016/0003-2697(68)90154-1
- Kragh KN, Alhede M, Kvich L, Bjarnsholt T. 2019. Into the well-A close look at the complex structures of a microtiter biofilm and the crystal violet assay. *Biofilm.* 1:100006. doi:10.1016/j.biofilm.2019.100006
- Lamas Ferreira JL, Álvarez Otero J, González González L, Novoa Lamazares L, Arca Blanco A, Bermúdez Sanjurjo JR, Rodríguez Conde I, Fernández Soneira M, de la Fuente Aguado J. 2017. *Pseudomonas aeruginosa* urinary tract infections in hospitalized patients: mortality and prognostic factors. *PLoS ONE.* 12:e0178178–13. doi:10.1371/journal.pone.0178178
- Langendonk RF, Neill DR, Fothergill JL. 2021. The building blocks of antimicrobial resistance in *Pseudomonas aeruginosa*: implications for current resistance-breaking therapies. *Front Cell Infect Microbiol.* 11:665722–665759. doi:10.3389/fcimb.2021.665759.
- Lara-Isla A, Medina-Polo J, Alonso-Isa M, Benítez-Sala R, Sopenña-Sutil R, Justo-Quintas J, Gil-Moradillo J, González-Padilla DA, García-Rojo E, Passas-Martínez JB, et al. 2017. Urinary infections in patients with catheters in the upper urinary tract: microbiological study. *Urol Int.* 98:442–448. doi:10.1159/000467398
- Lee KH, Park SJ, Choi SJ, Uh Y, Park JY, Han KH. 2017. The influence of urinary catheter materials on forming biofilms of microorganisms. *J Bacteriol Virol.* 47:32–40. doi:10.4167/jbv.2017.47.1.32
- Lister PD, Wolter DJ, Hanson ND. 2009. Antibacterial-resistant *Pseudomonas aeruginosa*: clinical impact and complex regulation of chromosomally encoded resistance mechanisms. *Clin Microbiol Rev.* 22:582–610. doi:10.1128/CMR.00040-09
- Luther MK, Parente DM, Caffrey AR, Daffinee KE, Lopes VV, Martin ET, Laplante KL. 2018. Clinical and genetic risk factors for biofilm-forming *Staphylococcus aureus*. *Antimicrob Agents Chemother.* 62:e02252–e02317 doi:10.1128/AAC.02252-17
- Ma L, Conover M, Lu H, Parsek MR, Bayles K, Wozniak DJ. 2009. Assembly and development of the *Pseudomonas aeruginosa* biofilm matrix. *PLoS Pathog.* 5:e1000354. doi:10.1371/journal.ppat.1000354
- Madsen JS, Lin YC, Squyres GR, Price-Whelan A, Torio A de S, Song A, Cornell WC, Sørensen SJ, Xavier JB, Dietrich LEP. 2015. Facultative control of matrix production optimizes competitive fitness in *Pseudomonas aeruginosa* PA14 biofilm models. *Appl Environ Microbiol.* 81:8414–8426. doi:10.1128/AEM.02628-15
- Mattick JS. 2002. Type IV pili and twitching motility. *Annu Rev Microbiol.* 56:289–314. doi:10.1146/annurev.micro.56.012302.160938
- Mirzahosseini H, Haddadi Fishani M, Morshedi K. Meta-Analysis of Biofilm Formation, Antibiotic Resistance Pattern, and Biofilm-Related Genes in *Pseudomonas aeruginosa* Isolated from Clinical Samples. *Microbial Drug Resistance.* 2020;26. doi:10.1089/mdr.2019.0274
- Kumari M, Khurana S, Bhardwaj N, Malhotra R, Purva M. 2019. Pathogen burden & associated antibiogram of *Pseudomonas* spp. in a tertiary care hospital of India. *Indian J Med Res.* 149:295–298. doi:10.4103/ijmr.IJMR_14_18
- Mulcahy LR, Isabella VM, Lewis K. 2014. *Pseudomonas aeruginosa* biofilms in disease. *Microb Ecol.* 68:1–12. doi:10.1007/s00248-013-0297-x
- Nolan LM, McCaughey LC, Merjane J, Turnbull L, Whitchurch CB. 2020. ChpC controls twitching motility-mediated expansion of *Pseudomonas aeruginosa* biofilms in response to serum albumin, mucin and oligopeptides. *Microbiology (Reading).* 166:669–678. doi:10.1099/mic.0.000911
- O'Toole GA. 2011. Microtiter dish biofilm formation assay. *J Vis Exp.* 30;(47):2437. doi:10.3791/2437.
- O'Toole GA, Kolter R. 1998. Flagellar and twitching motility are necessary for *Pseudomonas aeruginosa* biofilm development. *Mol Microbiol.* 30:295–304. doi:10.1046/j.1365-2958.1998.01062.x
- Pinzon NM, Ju L. 2009. Analysis of rhamnolipid biosurfactants by methylene blue complexation. *Appl Microbiol Biotechnol.* 82:975–981. doi:10.1007/s00253-009-1896-9

- Pratt LA, Kolter R. 1998. Genetic analysis of *Escherichia coli* biofilm formation: roles of flagella, motility, chemotaxis and type I pili. *Mol Microbiol.* 30:285–293. doi:10.1046/j.1365-2958.1998.01061.x
- Reichhardt C, Jacobs HM, Matwischuk M, Wong C, Wozniak DJ, Parsek MR. 2020. The Versatile *Pseudomonas aeruginosa* biofilm matrix protein CdrA promotes aggregation through different extracellular exopolysaccharide interactions. *J Bacteriol.* 202:1–9. doi:10.1128/JB.00216-20
- Reichhardt C, Wong C, da Silva DP, Wozniak DJ, Parsek MR. 2018. CDRA interactions within the *Pseudomonas aeruginosa* biofilm matrix safeguard it from proteolysis and promote cellular packing. *MBio.* 9:1–12. doi:10.1128/mBio.01376-18
- Römling U, Galperin MY, Gomelsky M. 2013. Cyclic di-GMP: the first 25 years of a universal bacterial second messenger. *Microbiol Mol Biol Rev.* 77:1–52. doi:10.1128/mnbr.00043-12
- Ryder C, Byrd M, Wozniak DJ. 2007. Role of polysaccharides in *Pseudomonas aeruginosa* biofilm development. *Curr Opin Microbiol.* 10:644–648. doi:10.1016/j.mib.2007.09.010
- Sarkar S. 2020. Release mechanisms and molecular interactions of *Pseudomonas aeruginosa* extracellular DNA. *Appl Microbiol Biotechnol.* 104:6549–6564. doi:10.1007/s00253-020-10687-9
- Saxena S, Banerjee G, Garg R, Singh M. Comparative Study of Biofilm Formation in *Pseudomonas aeruginosa* Isolates from Patients of Lower Respiratory Tract Infection. *J Clin Diagn Res.* 2014;8(5):DC09–11. doi:10.7860/JCDR/2014/7808.4330
- Shigemura K, Arakawa S, Sakai Y, Kinoshita S, Tanaka K, Fujisawa M. 2006. Complicated urinary tract infection caused by *Pseudomonas aeruginosa* in a single institution (1999–2003). *Int J Urol.* 13:538–542. doi:10.1111/j.1442-2042.2006.01359.x
- Stepanović S, Ćirković I, Ranin L, Švabić-Vlahović M. 2004. Biofilm formation by *Salmonella* spp. and *Listeria monocytogenes* on plastic surface. *Lett Appl Microbiol.* 38:428–432. doi:10.1111/j.1472-765X.2004.01513.x
- Suriyanarayanan T, Qingsong L, Kwang LT, Mun LY, Truong T, Seneviratne CJ. 2018. Quantitative proteomics of strong and weak biofilm formers of *enterococcus faecalis* reveals novel regulators of biofilm formation. *Mol Cell Proteomics.* 17:643–654. doi:10.1074/mcp.RA117.000461
- Tellis RC, Mososabba MS, Roche RA. 2017. Correlation between biofilm formation and antibiotic resistance in uropathogenic *Pseudomonas aeruginosa* causing catheter associated urinary tract infections. *Eur J Pharm Med Res.* 4:248–252.
- Tetz GV, Artemenko NK, Tetz VV. 2009. Effect of DNase and antibiotics on biofilm characteristics. *Antimicrob Agents Chemother.* 53:1204–1209. doi:10.1128/AAC.00471-08
- Thi MTT, Wibowo D, Rehm BHA. 2020. *Pseudomonas aeruginosa* biofilms. *IJMS.* 21:8625–8671. doi:10.3390/ijms21228671
- Thibeaux R, Kainiu M, Goarant C. 2020. Biofilm formation and quantification using the 96-microtiter plate. *Methods Mol Biol.* 2134:207–214. doi:10.1007/978-1-0716-0459-5_19
- Valentini M, Filloux A. 2016. Biofilms and Cyclic di-GMP (c-di-GMP) signaling: lessons from *Pseudomonas aeruginosa* and other bacteria. *J Biol Chem.* 291:12547–12555. doi:10.1074/jbc.R115.711507
- Vipin C, Mujeeburahiman M, Arun AB, Ashwini P, Mangesh SV, Rekha PD. 2019. Adaptation and diversification in virulence factors among urinary catheter-associated *Pseudomonas aeruginosa* isolates. *J Appl Microbiol.* 126:641–650. doi:10.1111/jam.14143
- Webb JS, Thompson LS, James S, Charlton T, Tolker-Nielsen T, Koch B, Givskov M, Kjelleberg S. 2003. Cell death in *Pseudomonas aeruginosa* biofilm development. *J Bacteriol.* 185:4585–4592. doi:10.1128/JB.185.15.4585-4592.2003
- Wu J, Xi C. 2009. Evaluation of different methods for extracting extracellular DNA from the biofilm matrix. *Appl Environ Microbiol.* 75:5390–5395. doi:10.1128/AEM.00400-09
- Xu ZG, Gao Y, He JG, Xu WF, Jiang M, Jin HS. 2015. Effects of azithromycin on *Pseudomonas aeruginosa* isolates from catheter-associated urinary tract infection. *Exp Ther Med.* 9:569–572. doi:10.3892/etm.2014.2120
- Zhang W, Sun J, Ding W, Lin J, Tian R, Lu L, Liu X, Shen X, Qian PY. 2015. Extracellular matrix-associated proteins form an integral and dynamic system during *Pseudomonas aeruginosa* biofilm development. *Front Cell Infect Microbiol.* 5:10–40. doi:10.3389/fcimb.2015.00040.
- Zheng S, Bawazir M, Dhall A, Kim HE, He L, Heo J, Hwang G. 2021. Implication of surface properties, bacterial motility, and hydrodynamic conditions on bacterial surface sensing and their initial adhesion. *Front Bioeng Biotechnol.* 9:643722–643722. doi:10.3389/fbioe.2021.643722.

Appendices

AU	Artificial Urine
CAUTI	Catheter Associated Urinary Tract infections
CLSM	Confocal Laser Scanning Electron Microscope
CV	Crystal Violet
E-SEM	Environmental- Scanning Electron Microscope
eDNA	extracellular DNA
LB	Luria Broth
NA	Natural Urine
TSB	Tryptone Soya Broth
T4P	Type 4 pili
OD	Optical density
ODc	Cutt-off OD value
UTI	Urinary Tract Infection